Nuclear Instruments and Methods in Physics Research B52 (1990) 237-333
North-Holland

An ultra-clean microprobe ion source for atomic mass spectrometry

S. Matteson, J.L. Duggan, D. Marble, F.D. McDaniel, D.L. Weathers and D.K. Wilson
Center for Materials Characterization/Physics University of North Texas, Denton, Texas 76203-5368, USA

J.M. Anthony and R.L. Beavers
Texas Instruments Incorporated, Dallas, Texas 75265, USA

The design and initial implementation of an ultra-clean microprobe ion source (Chimera), which is under construction at the University of North Texas in collaboration with Texas Instruments, is presented. The source, which is intended for trace impurity analysis of stable isotopes, combines the features of existing secondary ion mass spectrometry (SIMS) microprobe instruments with the molecular discrimination and single-ion detection capabilities of accelerator mass spectrometry (AMS). Issues of cesium ion microbeam formation and cleanliness, secondary ion collection and transmission efficiency are discussed. Novel features of the Chimera include high-resolution magnetic analysis of the primary Cs^+ ion beam ($m/\Delta m > 200$), high-purity silicon slits and an ultra-high vacuum analysis chamber with unique silicon-based extraction optics and sample holder.

1. Introduction

The application of secondary ion mass spectrometry (SIMS) to materials science problems has become highly developed in the last decade [1]. Investigators have found, however, that SIMS suffers from molecular and charge state interferences that limit the sensitivity of the technique in these unfortunately frequent instances.

Moreover, the presence of numerous molecular species complicates the unambiguous identification of trace elemental impurity species. Accelerator mass spectrometry (AMS), which utilizes tandem acceleration and its concomitant stripping and Coulombic explosion of molecules, provides a truly *atomic* mass spectrometry [2].

At the University of North Texas (UNT) we have configured a 3 MV tandem accelerator (NEC 9SDH-Pelletron) into an AMS system, incorporating two high-resolution magnetic mass spectrometers, a high-resolution electrostatic energy analyzer, femto-ampere current measurement and single-ion counting, under computer control. The system and the detection performance are described in detail elsewhere [3,4]. The UNT accelerator spectrometer has demonstrated the capability of 13 decades of dynamic range in mass scans; molecular ions have been shown to be rejected to better than one part in 10^{12}.

The present ion source consists of a high-intensity focussed cesium plasma of a conventional design. The source is manufactured by National Electrostatics Corporation and is called a SNICS source. Baseline detection limits in silicon were established by the insertion of a sample of float-zone-refined single-crystal silicon of ultra-high purity. The authors found that ion beams of intensities indicative of impurity levels much higher than are known to exist in the material were present. In particular, the first transition elements are of interest. In fig. 1 is plotted the intensity of masses 50 u to 60 u, normalized to the total silicon ion yield. These relative intensities are equivalent to concentrations on the order of 10^{16} cm^{-3} (200 ppb). The origin of these spurious impurities is believed to be contamination of the cesium plasma from the stainless steel of the ion source itself. The SNICS source exhibits another common but equally undesirable tendency of a SIMS-AMS source: the so-called memory effect. Analysis of a material containing a given impurity (^{12}C in a silicon matrix, for example) following analysis of another sample with a matrix that contains a high concentration of the erstwhile impurity (such as graphite) will reveal a persistent residual high level of contamination unrelated to the actual impurity levels in the later-analyzed specimen. At the very high sensitivities afforded by AMS, analyses of samples of unknown but high purity can be compromised by the cross-contamination by impurities from a standard specimen with impurity levels barely sufficient for tuning the ion beam.

Additional disadvantages of sources of the design commonly used in AMS are the lack of precise control of the position of the ion beam on the sample and the inability of performing meaningful depth profiling or surface analysis. Both of these capabilities, which are commonplace in SIMS instrumentation, require a well-focussed primary ion beam that can be scanned across

0168-583X/90/$03.50 © 1990 - Elsevier Science Publishers B.V. (North-Holland)

an area to produce a flat-bottomed sputter crater that interrogates various buried layers in a controlled manner.

The difficulties presented above distinguish the present enterprise from conventional AMS, which generally strives for a limited dynamic range (~ 3 decades in the case of $^{14}C/^{12}C$ chronology) of a few isobars but with great precision and reproducibility. The great strength of AMS is realized in radioisotopic mass spectrometry, since rarely does the ion source itself contribute significantly to the isotopic ion beam. This is not the case, however, in the application of AMS to trace stable isotopic mass spectrometry where numerous sources of spurious signal can exist.

2. System overview

The stringent demands made upon the ion source of this work require a design that may sacrifice simplicity for cleanliness, and compactness for flexibility. The ion source must be of a new form that adequately adapts SIMS to the requirements of AMS. The name given to this source, Chimera, recalls the mythological creature recounted to be formed of disparate parts. The name is also an acronym for CHemical Identification by Mass and Energy Resolution and Analysis.

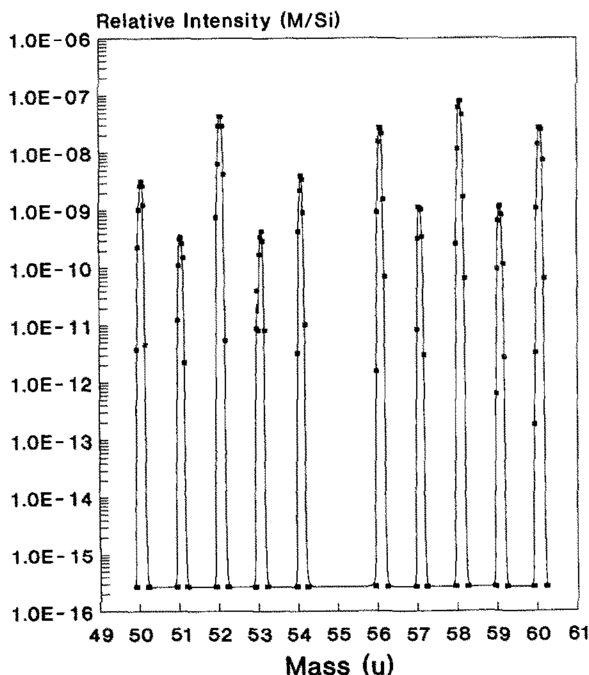

Fig. 1. AMS mass scan of first transition metal series, normalized to silicon. The high levels of iron and nickel are evidence of contamination from the ion source itself.

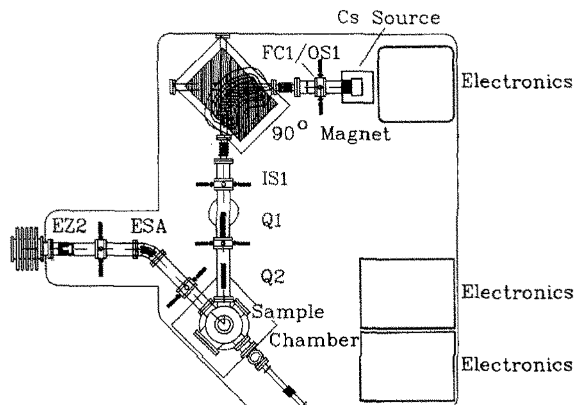

Fig. 2. Schematic of the ultra-clean ion source, Chimera. Primary ions are produced in a cesium thermal ionization source (Cs source), accelerated to approximately 10 keV, and focussed on the object slits and Faraday cup assembly (FC1/OS1). The Cs^+ ion beam is mass analyzed in a 90° double-focussing magnet and imaged on slits (IS1). The primary ion beam then is demagnified and scanned by means of quadrupole multiplets Q1 and Q2. The primary beam then sputters atoms and molecules from the sample surface; the secondary ions are extracted, focussed on field apertures, energy analyzed by an electrostatic analyzer (ESA) and focussed by an einzel lens (EZ2) on the object slits of the injection magnetic spectrometer of the accelerator (not shown). The secondary ions undergo a second acceleration of approximately 50 keV after they leave the source, so that the total ion energy is near 70 keV, which matches the injection optics of the tandem accelerator.

Fig. 2 gives a schematic overview of the Chimera. The overall dimensions of the source are approximately three meters wide by three meters long by two meters high. The source consists of a primary ion source (Cs^+), a 90° primary magnetic spectrometer, microbeam forming and scanning optics, and an ultra-high vacuum sample chamber (capable of 10^{-11} Torr) with secondary ion extraction optics and a sample vacuum interlock. The beamline configuration of the source permits the use of well-tested beam forming optics and novel construction technology. The source is enclosed in an equipotential chassis, which rests on a 12 mm thick steel deck supported by thirty high-voltage ceramic insulators. The chassis is maintained at a source bias that matches the injection optics of the tandem accelerator (−50 kV).

Mains power is supplied to the enclosure by two isolation transformers delivering the necessary power to drive the turbomolecular pumps, backing pumps, high-current magnet, control electronics and power supplies in the Chimera. Various functions of the source are computer controlled via an electromagnetic interference (EMI) shielded personal computer (PC) that communicates with a similar device in the control room via an

IEEE-488 bus, which has been extended by means of a fiber optical data link. Fiber optical analog links, as well as dedicated high-speed digital data fiber optical channels, are also utilized for special functions such as ion-beam-position synchronization during raster scanning. The sample is manipulated by piezo-electric "inch worm" micromanipulators under computer control. The surface of the specimen is viewed by means of a long working distance microscope (WD > 2 m) and a high-resolution solid state camera that is monitored remotely in the control room.

The vacuum system is constructed of electropolished stainless steel with all-metal static seals, in order to obtain ultimate pressures of less than 10^{-8} Torr throughout the system. The sample chamber is a modification of a standard surface analytic chamber that routinely reaches pressures of less than 10^{-10} Torr. The chamber is pumped by a 500 l/s turbomolecular pump backed by a 150 l/s turbomolecular pump and mechanical roughing pump. This arrangement takes full advantage of the high compression ratio of the turbomolecular pump. A cryogenic surface and titanium sublimator assist in the pumping of hydrogen and other gaseous impurities. The partial pressures of residual gases are determined by a quadrupole mass residual gas analyzer. The use of turbomolecular pumps permits the dosing of the sample surface with various gases, such as oxygen, in order to increase the secondary negative ion emission of molecular species that contain that impurity, such as FeO^- [5]. The importance of a low ultimate pressure, on the other hand, can be appreciated by considering the effect of residual oxygen or carbon in the vacuum that impinges on the sputtering surface and acts as an extra-specimen source of these impurities. Thus, attaining an ultra-high vacuum is essential in securing the necessary sensitivity for these and other residual gas elements.

3. Primary ion beam purity

As discussed above, the contamination of the cesium in the ion source of the SNICS type is believed to be a major contribution to the background sensitivity limit of common AMS source designs. In the Chimera, a modified cesium thermal ionization source (originally manufactured by General Ionex Corporation) produces a positive cesium ion beam of from 10–100 μA by thermionic emission from a tungsten frit held at about 1000°C. The crossover of the ion beam in a modification of the original source design forms a small virtual source at the position of the object slits of a double focussing sector magnet (manufactured by the Magnecoil Corporation). The optics of this magnet design are such as to produce a real image of unit magnification at the position of the image slits [6].

Anthony et al. have shown that the cesium ion beam from such a source is likely to contain impurity beams at the part-per-million level [5]. Fig. 3 shows the result of a similar mass scan of the primary ion beam of the Chimera in the mass range up to ^{133}Cs. Note that there are indeed other low-level ion beams in the unanalyzed beam, particularly of other alkali metals. Please note also the high resolution of the mass peaks and the large separation of the impurity beams. This mass scan demonstrates that the 90° sector magnet provides the required impurity rejection in the primary ion beam.

The primary ion beam must, at some point, be

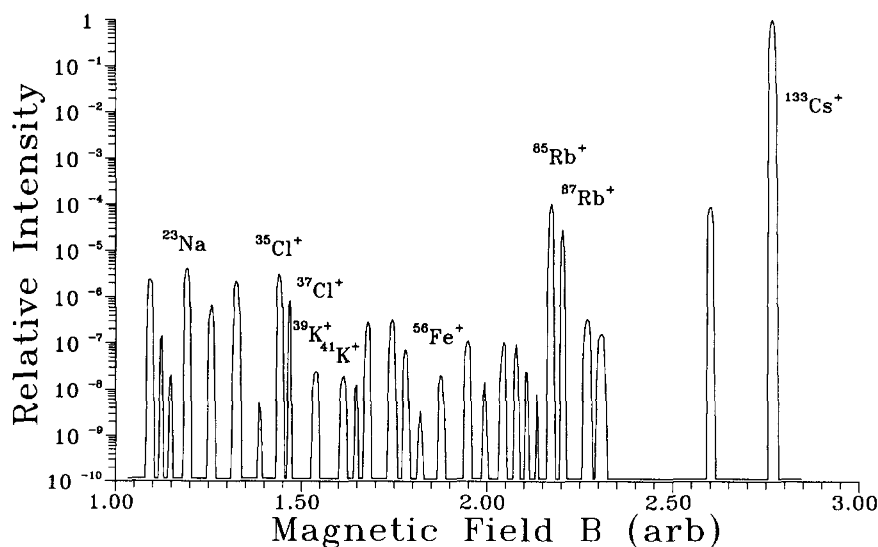

Fig. 3. Normalized mass scan of the primary ion beam. Note the relative isolation of the mass 133 u peak of Cs^+. Thus, the purity of the primary ion beam is assured. The variable width of the peaks is an instrumental effect.

collimated. The material from which the collimator or slit assembly is formed will be sputtered by the ion beam. If we consider beam current to be 100 μA and that 90% of the ion beam passes through the collimator without striking one of the collimator surfaces while about 1% of the ion beam strikes the edge of the collimator and the remainder the front surface, the collimator knife edge will be sputtered at a rate of $N = SI/e$, with S the sputter yield and I the ion current that actually strikes the slit edge. The sputter yield depends strongly on the angle, but yields of from $S = 1$ to 10 are conservative estimates. Thus under these conditions one expects an erosion rate of the surface of from about 6×10^{12} atoms s^{-1} to 6×10^{13} atoms s^{-1}.

If the pristine sample surface is located a distance r from the collimator and the collimator has an opening of width w, then the average rate of deposition per unit area on the surface of the sample is proportional to $w/\pi r^3$. An inverse square dependence arises from the solid angle of the sample surface, while an additional approximate factor of $w/\pi r$ results from the cosine dependence of the yield of sputtered atoms [7]. At a distance of 1 cm from a 1 mm collimator we estimate the contamination rate to be from about 1% to 10% of a monolayer per second while at a distance of one meter from the collimator the rate drops to a value of from 10^{-8} to 10^{-7} monolayer per second. While the precise values of these estimates may be questionable, the order of magnitude is realistic. The conclusion is clear: the collimator must be of a material that is innocuous. We have chosen silicon for the collimator material rather than a metal, since silicon has a relatively low sputtering yield, is highly pure and is a constituent of many of the sample matrices. Moreover, the collimator/slit must be placed a large distance (> 100 cm) from the sample in order to keep the contamination low. In addition, by avoiding a direct line of sight from the collimator to the sample surface, the contaminating effect of the collimator can be further reduced. Also, by use of a finely focussed beam, the width of the collimator w can be further reduced, lowering the deposition rate to acceptably low levels. In the case of samples for which silicon is an impurity of interest and for which the sensitivity is inadequate, germanium can be substituted as the collimator material. Thus, interfering impurity contamination from the collimator can be reduced to a negligible level, well below 10^{-12} monolayer s^{-1}.

4. Memory effect reduction

The memory effect or cross contamination is a more formidable problem than those considered above, because of the proximity of the electrode surfaces to the sputtering sample. The secondary negative ions must, of course, be collected without their impact upon a solid surface. This can be achieved straightforwardly. The neutral sputtered species, however, not only deposit on first-wall surfaces but cause redeposition of previously sputtered material onto the pristine sample. One can easily show that the deposition rate of sputtered neutral material is proportional to the inverse square of the distance from the sample surface to the first electrode surface. Moreover, the rate of redeposition will also have the same dependence on the electrode–sample distance. If this distance is approximately 2 cm and the sputter yield of the low-energy neutrals is as large as 0.1, then one can expect a redeposition fraction (monolayer of contamination/monolayer of material removed) of previously deposited material of about 10^{-5}. This estimate assumes an impurity coverage of 10% and an erosion rate of the sample of about one monolayer per second over an area of 1 mm^2. This corresponds to a beam current of about 1 μA. Increasing the total beam current, but keeping the sputter region the same size, does not alter the relative contamination levels, since both the erosion rate and redeposition rate are increased by like factors. By use of a smaller beam spot, and therefore a lower total neutral sputter yield for the same erosion rate, the relative redeposition rate can be reduced. Alternatively, the aperture above the sample surface can be enlarged, so that a larger fraction of the neutral sputtered material escapes to more distant surfaces. But a large aperture and distant electrodes are generally inconsistent with efficient charge collection. Moreover, the mean time to 10% coverage in the case presented above is only about 3.5 h with a 1 mm^2 raster area, while an area 100 μm × 100 μm will require 350 h before reaching 10% coverage. If standard samples that contain less than 1 ppm (5×10^{16} cm^{-3}) of the impurities of interest, then the memory effect will be insignificant for many hours of analysis. Ease of exchange and of cleaning are important operational issues that must be comprehended in the design of an instrument that will remain consistently sensitive.

Early designs of SIMS instruments had optical elements that were on the order of about 1 mm from the sample surface and difficult to remove. Thus, the level of the problem as discussed in the previous paragraph was exacerbated by a factor of about 400 in those instruments. The design of the Chimera extraction optics, however, permits good secondary ion collection with minimal cross contamination. The sample holder, which accommodates twenty-five samples per load, is fabricated from 1.25 mm thick silicon with twenty-five 3.0 mm diameter holes arranged in concentric circular arrays. The samples, which routinely may be as large as 7 mm in diameter, span the apertures in the sample holder. The well formed by the hole and sample form an immersion lens for the secondary ions that leave the surface of the sample. The aspect ratio of this cylindrical depression limits the direction of the neutral

sputtered species to a cone of half-angle about 34° to the normal. A silicon baffle with a ~ 5 mm diameter hole positioned approximately 1 mm above the sample holder shields all the samples awaiting analysis from contamination. In combination with the first electrode, an extraction potential is established that causes a crossover of the ions to occur at about 1 to 2 mm above the sample surface. Behind the extraction electrode, which is at the ion source chassis potential, is a second electrode that has a larger aperture and negative bias. This electrode in conjunction with a final electrode constitutes an einzel lens system. Computer simulations of the electric fields and ion trajectories computed by the code SIMION 3.1 [8] for several proposed geometries has permitted the design of an extraction system for which the ions will not impact any surface and form a real image of the sample surface with a magnification of about 3 ×. This latter feature allows the rejection of ions that arise from the edges of the sputter crater by blocking with a post-extraction collimator. In this way one is able to enhance the resolution of sputter depth profiling and to extend the dynamic range of the analysis of a given sample.

The extraction optics are fabricated from flat silicon (or germanium) wafers of semiconductor electronics-grade material. The necessary apertures are laser machined in the material. The first surface can be cooled to cryogenic temperatures, which we have observed to reduce the background level and memory effect for volatile species. The capability for internal baking and outgassing assures that the layers deposited on the first surfaces are stable and not easily transferred to the sample by an ion-induced desorption of physisorbed atoms. The optics are attached to a large-diameter flange, so that they can be easily removed and a second set rapidly installed, while the first is being cleaned. It is anticipated that, except for matrix constituents, no significant redeposition will occur in normal operation. However, when changing matrices, for example from silicon to steel and back to silicon, care must be exercised to provide fresh optics for the material or group of materials of interest.

5. Microbeam optics

Precise control of the primary ion beam is essential to attainment of a clean ion source. By detecting secondary ions in the AMS spectrometer in coincidence with or in correlation to the position on a sample surface of a scanned microbeam, one can form a two-dimensional image of the lateral distribution of impurities in a sample. Moreover, by scanning the primary ion microprobe repeatedly over the same region, one can sputter a crater and thereby permit the interrogation of the impurity concentration as a function of depth. These

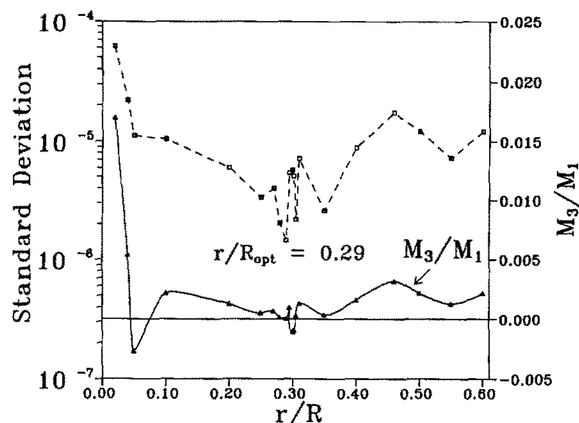

Fig. 4. The relative error between the computed electrostatic potential distribution and ideal dipole field for cylindrical arrangement of eight electrodes as a function of electrode radius to bore radius. Also shown is the normalized sextupole moment of the field. The optimum rod to bore ratio is ~ 0.3.

capabilities are predicated on the ability to form and control a micrometer-size cesium ion beam.

The Chimera makes extensive use of octupole, i.e. eight electrode, arrangements of cylindrical rods. This arrangement can be fabricated with excellent accuracy and allows the realization of various optical elements with very similar mechanical designs. These include electrostatic dipole deflectors, quadrupole lens and octupole corrector elements. The added complication of the eight potentials is necessary in order to achieve low operating potentials and low aberrations. Scherzer has clearly demonstrated that the spherical aberration of an axially symmetric lens system cannot be negative; the aberration, moreover, has been conjectured to be positive definite [9]. Fishkova and Yavor and have shown, on the other hand, that octupole correctors used in conjunction with quadrupole/octupoles can be configured in optical systems with zero spherical aberration [10,11].

An essential element of the Chimera primary ion microbeam formation is the dipole element. Rather than use two sets of parallel plates separated in space, we will utilize a set of eight round rods properly energized so as to yield a dipole field of any desired orientation. This arrangement was first reported by Idesawa in 1979 [12]. Fig. 4 illustrates the deviation of the potential field of the dipole/octupole from an ideal dipole field, as a function of the ratio of the radius r to the bore radius R. The deviation was calculated as the mean variance of the fields, averaged over the circular region of radius less than $R/2$ in the dipole/octupole arrangement, which is shown in fig. 5. Laplace's equation was solved for various geometries using SIMION to generate the data. The small scatter in the data points reflects the digitization error in approximating rods of circular cross

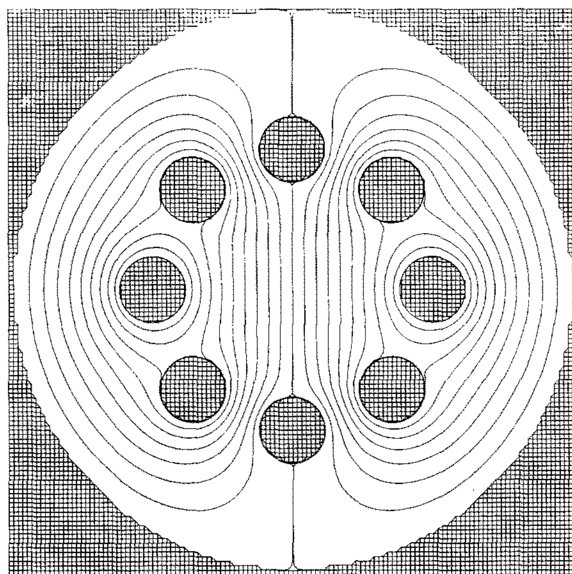

Fig. 5. Cross section view of "octupole" arrangement for optimum dipole field, with equipotential contours.

section by polygonal cross sections in Cartesian coordinates. It can be easily observed from the figure that for r/R ratios greater than about 0.3 an excellent approximation to a dipole field can be achieved. Indeed, the error in this configuration is less than 25% of that of the commonly used eight-segment split-tube dipole/octupole arrangement [13]. The necessary ratio of the potentials V_1/V_2 to permit superpositioning of the dipole fields is $1/\sqrt{2}$. In fig. 4 the ratio of sextupole moment to dipole moment of the potential distributions are also plotted versus the r/R ratio. The sextupole moment, the first harmonic in a multipole expansion of the field, vanishes for a value of $r/R = 0.29$. The value gives the lowest mean square deviation from the ideal dipole within a circle of $R/2$.

Fig. 2 schematically illustrates the microbeam formation. The ions emitted from the primary cesium source form an image 50–100 μm in diameter at the object slit of the magnet. The magnet then forms, with unit magnification, an image on its image slits. A quadrupole/octupole triplet forms a intermediate real image of magnification ~ 1/50. This image is very near the end of the lens. In order to achieve the necessary working distance, a final objective lens quadruple/octupole multiplet (with mid-lens deflection) images the beam on the sample. The astigmatism of the lens is utilized to form an elliptical spot on the sample that, because of the angle of incidence, will project as a circular beam spot. The combination of the two multiplets is in effect a zoom lens, permitting a wide latitude in primary beam optics. A special feature incorporated into the primary beam optics is the capability of radically reducing the beam spot intensity as well as size, well below that useful for sputtering or secondary ion emission, but quite adequate for the emission of secondary electrons. By the collection and amplification of the secondary electrons from the surface of the sample, the topography of the sample can be imaged in a manner similar to scanning electron microscopy. In this way one can align the ion beam with the region of interest to be analyzed without unduly altering the specimen.

6. Conclusion

The Chimera AMS–SIMS ion source at the University of North Texas is a versatile instrument uniquely adapted to the production of secondary ion beams from samples without the significant introduction of contamination by stable elemental impurities. The Chimera takes advantage of the power of AMS for molecular dissociation and single-ion detection as well as the best features of its predecessor ion microprobe instruments. The instrument incorporates several novel features to permit part-per-trillion analysis of stable isobars, including primary cesium ion mass separation, ultra-pure silicon collimators, advanced ion optics with electron and secondary ion imaging and depth profiling. The system is under computer control for efficient control, data acquisition and reduction. The Chimera ion source is a powerful and unique instrument that will be of great assistance in attacking many problems in the materials science of trace impurity–matrix interaction.

Acknowledgements

This work is supported in part by the National Science Foundation Grant no. DMR-8812331, the Office of Naval Research Grants no. N00014-89-J-1309 and no. N00014-89-J1344, Texas Instruments Incorporated, the State of Texas Higher Education Coordinating Board–Texas Advanced Technology Research Program, the Robert Welch Foundation and the University of North Texas Organized Research Fund. The authors gratefully acknowledge the technical assistance of Mr. T.J. Bennett and Ms. Susan M. Hemming.

References

[1] A. Benninghoven, R.J. Colton, D.S. Simons and H.W. Werner (eds.), Secondary Ion Mass Spectrometry SIMS V (Springer, Berlin, 1986).

[2] S. Matteson, D.K. Marble, L.S. Hodges, J.Y. Hajsaleh, A.M. Arrale, M.R. McNeir, J.L. Duggan, F.D. McDaniel and J.M. Anthony, Nucl. Instr. and Meth. B45 (1990) 575.

[3] J.M. Anthony, S. Matteson, J.L. Duggan, P.S. Elliott, D.L. Weathers, D. Marble and F.D. McDaniel, these Proceedings (AMS 5) Nucl. Instr. and Meth. B52 (1990) 493.

[4] F.D. McDaniel, S. Matteson, D.L. Weathers, D.K. Marble, J.L. Duggan, P.S. Elliott and D.K. Wilson, ibid., p. 310.

[5] J.M. Anthony, D.J. Donahue and A.J.T. Jull, Mat. Res. Soc. Symp. Proc. 69 (1986) 311.

[6] H.A. Enge, in: Focusing of Charged Particles, vol. 2, ed. A. Septier (Academic Press, New York, 1967) p. 203.

[7] M.J. Vasile, Phys. Rev. B29 (1984) 3785.

[8] D.A. Dahl and J.E. Delmore, SIMION PC/PS2 version 3.1 (Idaho National Engineering Laboratory, Idaho Falls, Idaho, 1987).

[9] O. Sherzer, Z. Phys. 101 (1936) 465.

[10] T.Ya. Fishkova and S.Ya. Yavor, Zh. Tekh. Fiz. 38 (1968) 686 [Sov. Phys. - Tech. Phys. 13 (1968) 514].

[11] L.A. Baranova and S.Ya. Yavor, Advances in Electronics and Electron Physics, vol. 76, ed. P.W. Hawkes (Academic Press, New York, 1989) p. 1.

[12] M. Idesawa, E. Goto, T. Soma and T. Sasaki, Proc. 15th Symp. on Electron, Ion and Photon Beam Technology, 1979, quoted by P.R. Thorton, in: Advanced Electronics and Electron Physics, vol. 54 (Academic Press, New York, 1980) p. 323.

[13] J. Kelly, T. Groves and H.P. Kuo, J. Vac. Sci. Technol. 19 (1981) 936.